XI International Conference on Computational Plasticity. Fundamentals and Applications
COMPLAS XI
E. Oñate, D.R.J. Owen, D. Peric and B. Suárez (Eds)

AN ELASTOPLASTIC-VISCOPLASTIC SOIL MODEL FOR CYCLIC LOADING

J. R. MARANHA*, ANA VIEIRA†

* Laboratório Nacional de Engenharia Civil (LNEC)
Av. do Brasil, 101, 1700 066, Lisbon, Portugal
e-mail: jmaranha@lnec.pt, www.lnec.pt

† Laboratório Nacional de Engenharia Civil (LNEC)
Av. do Brasil, 101, 1700 066, Lisbon, Portugal
e-mail: avieira@lnec.pt, www.lnec.pt

Key words: Computational Plasticity, Soil Mechanics, Cyclic Loading

Abstract. A mobile projection centre extension to an existing elastoplastic-viscoplastic soil model is presented in this work. In this formulation, the projection centre evolves according to the stress path experienced by the soil, approaching it during the loading process [1]. In this way, the elastic (within which the behaviour is elastic) and the viscous (within which the behaviour is non-viscous) nuclei, will move with the projection centre. These nuclei may have reduced dimensions and reproduce more realistically the inelastic and time dependent soil response under a larger set of stress paths. The proposed formulation is based on the continuous plasticity model with a viscous mechanism proposed by Kaliakin and Dafalias [2, 3]. The observed occurrence of creep deformation in stiff clays at small levels of deviatoric stress was one of the motivations for this work. It is important to note that the majority of numerical and laboratory studies of the effect of strain rate on the behaviour of soils usually refers to normally consolidated soils, and, as already reported by Hashiguchi and Okayasu [4], further theoretical and experimental studies on the time dependent behaviour of overconsolidated soils are needed.

In order to validate the proposed formulation a cyclic undrained triaxial test with unloading and reloading stages with creep was performed on a sample of a stiff Lisbon clay. The test was simulated using the described soil model and the results of both compared. This formulation significantly improves the reproduction of viscous strains associated with unloading stress paths such as those occurring, for example, in excavation works.

1 INTRODUCTION

Laboratory tests performed on a stiff clay from the Lisbon region (*Formação de Benfica* clays) showed the occurrence of creep strains at small deviatoric stress levels. These results were confirmed by local displacement transducers LVDTs [5], and motivated the study here presented. It is interesting to note that the vast majority of laboratory and numerical studies of

strain rate effects on soil behaviour refers to normally or lightly overconsolidated soils, with further studies of these effects on overconsolidated soils being necessary, as noted by Hashiguchi e Okayasu [4], both from the experimental and theoretical standpoints. The study presented below aims to contribute to overcome this shortcoming, highlighting some important aspects.

There are on the literature various types of models conceived to reproduce the time-dependent behaviour of soils. These models can be divided into two main groups, those that allow and those that do not allow the occurrence of viscous deformation inside the yield surface. Since, in the case of overconsolidated soils, stress paths can develop to a large extent within the yield surface, the later type of model is clearly limited in its applicability. Instead, continuous plasticity models, with an added viscous mechanism, such as the model proposed by Kaliakin and Dafalias [2,3], by enabling the occurrence of inelastic deformations inside the yield surface (called bounding surface), improve the reproduction of soil behaviour.

2 THE KALIAKIN AND DAFALIAS BOUNDING SURFACE ELASTOPLASTIC VISCOPLASTIC MODEL

2.1 Brief model description

The elastoplastic-viscoplastic soil model proposed by Kaliakin and Dafalias [2] is based on the existence of a bounding surface, with an elliptical shape in the space of the stress invariants *(p,q,θ)*, shown in Figure 1. The stress state $\boldsymbol{\sigma}$ is always inside or on the bounding surface, having an image on it, $\bar{\boldsymbol{\sigma}}$, defined by a radial projection from a centre **a**. In this particular model, the projection centre is fixed and located on the hydrostatic axis. The bounding surface only undergoes isotropic hardening. The position of the stress state on the line segment joining the projection centre to the image point on the bounding surface defines the variable $b = \|\bar{\boldsymbol{\sigma}} - \mathbf{a}\| / \|\boldsymbol{\sigma} - \mathbf{a}\|$. This varies between $b=\infty$, when the stress state matches the projection centre, and $b=1$, on the bounding surface.

A basic assumption of this model is the additive decomposition of the inelastic deformation rate into a plastic component and a viscoplastic component. The directions of the plastic and viscoplastic deformation rates are given by derivative of the yield function relatively to the stress state on the image point, $\bar{\boldsymbol{\sigma}}$. There are two surfaces implicitly defined associated to each of the inelastic mechanisms. The first one defines the boundary beyond which plastic deformations can occur (if the loading condition is also verified) represented by the constant s_p, such that $b \le s_p/(s_p - 1)$. The second surface defines the boundary outside which viscous deformation occur and is defined by the constant s_v. That means that viscoplastic deformations occur only if $b \le s_v/(s_v - 1)$. Both surfaces are homothetic relatively to the bounding surface. The overstress defined as $\hat{\delta} = \|\boldsymbol{\sigma} - \hat{\boldsymbol{\sigma}}\|$ controls the magnitude of viscoplastic strain rate. $\hat{\boldsymbol{\sigma}}$ is the in intersection point between the line joining the projection centre and the stress point, and the viscous nucleus.

The plastic modulus, that determines incremental elastoplastic stifness is interpolated from its value on the image point, by means of variable *b*, so that a continuous monotonic transition

from an infinite value (elastic incremental stiffness) on the surface $b = s_p/(s_p - 1)$ to a corresponding value on the bounding surface (conventional elastoplastic stiffness).

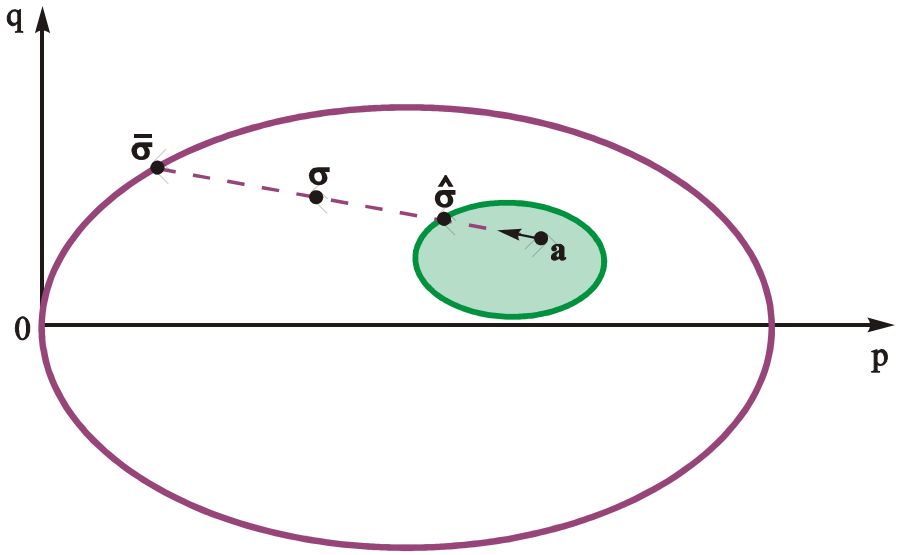

Figura 1: Bounding surface model.

The model was implemented in the explicit finite difference software FLAC. Details of this implementation can be found in [5,6].

2.2 Laboratory tests numerical modelling

The described model has enabled the reproduction of a set of three creep tests performed on *Formação de Benfica* stiff clays. The tests were triaxial undrained under constant mean stress after being isotropically consolidated to different effective mean stresses. The imposed loading sequence alternated steps of relatively high strain rate with 24 hours creep stages. This adjustment was initially achieved with a different set of model constants for each test, and, after a modification of the overstress function, by introducing a new parameter related with the viscous behaviour, the whole set of tests were adjusted using a single set of parameters [7]. The modified overstress function defining the magnitude of the viscous strain rates is given by

$$\phi = \frac{1}{V}\exp\left(\alpha\frac{J}{IN}\right)\left(\frac{\hat{\delta}}{r\left(\frac{s_v - 1}{s_v}\right)}\right)^n . \tag{1}$$

2.3 Limitations of the model

Although this model has been able to reproduce many of the relevant aspects of the viscous behaviour of soils, it still has some shortcomings. Figures 2 and 3 illustrate some of these

shortcomings. In the case of an overconsolidated clay, after the sedimentation process and associated creep, the stress state is at point A (apparent overconsolidation), soil undergoes unloading due to the erosion of the superficial layers (process which corresponds to a genuine overconsolidation process), and the final stress state point is B. Stress states A and B correspond to equilibrium situations, on which the creep strains have already occurred, and as such, are on the boundary of the viscous nucleus represented in Figures 2 and 3 as green shaded ellipses. The unloading stage from A to B, in the original model with the fixed projection centre over the hydrostatic axis, does not produce any creep (viscous) strains, because the corresponding stress path is now entirely included in the viscous nucleus (Figure 2). On the other hand, in the formulation now proposed, which admits the existence of a mobile projection centre (which implies a mobile viscous nucleus), creep strains will take place as long as the stress path AB is sufficiently long to cross the viscous nucleus.

Assuming the sample is sheared undrained from a state of isotropic consolidation, as was shown above, no creep deformations would occur within the surface s_v, according to the original model. However, it was observed that creep strains occurred from the earliest stress stages (low deviatoric stress), which is inconsistent with this model. This inconsistency can be eliminated by assuming that the projection centre (and the corresponding viscous nucleus) can move, as illustrated in Figure 3. The concept is equivalent to that proposed in two surface elastoplastic models. These, however, do not take into account the viscous behaviour. As long as the size of the viscous nucleus is sufficiently small, creep strains may occur at any point, inside the bounding surface.

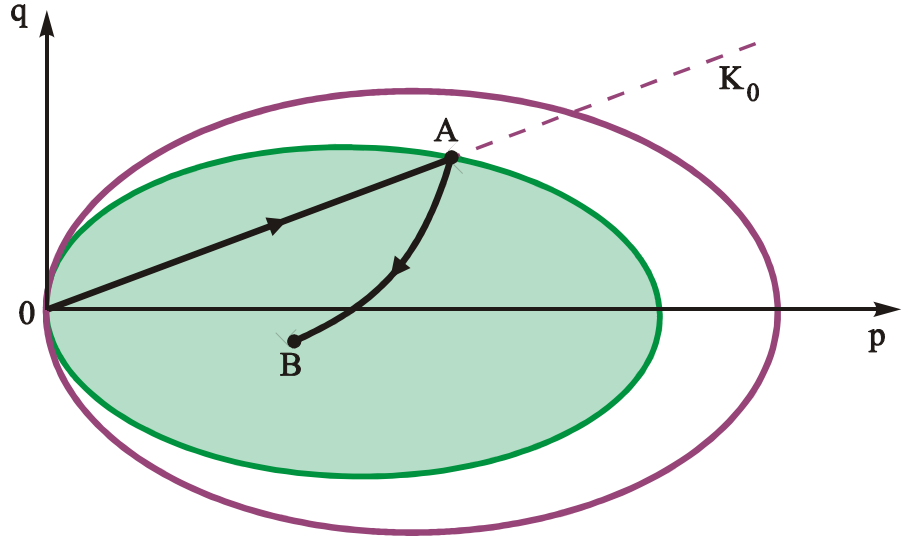

Figure 2 : Overconsolidation process in the original model (fixed projection centre).

In overconsolidated soils which have been stabilized in terms of creep, it would be necessary, according to the original model, to use a viscous nucleus large enough to accommodate the *in situ* stress states. Because, inside this nucleus no viscous strains may occur, this contradicts the results of the described tests. This contradiction may be eliminated by adopting a mobile projection centre defining a viscous nucleus of reduced dimension.

In the same way that the two surface models incorporate a mobile elastic domain in order to better represent the variation of the elastoplastic stiffness with the loading direction, it may

be assumed that the same principle applies to the viscous behaviour. The use of mobile viscoplastic potentials in metal models is well known [8].

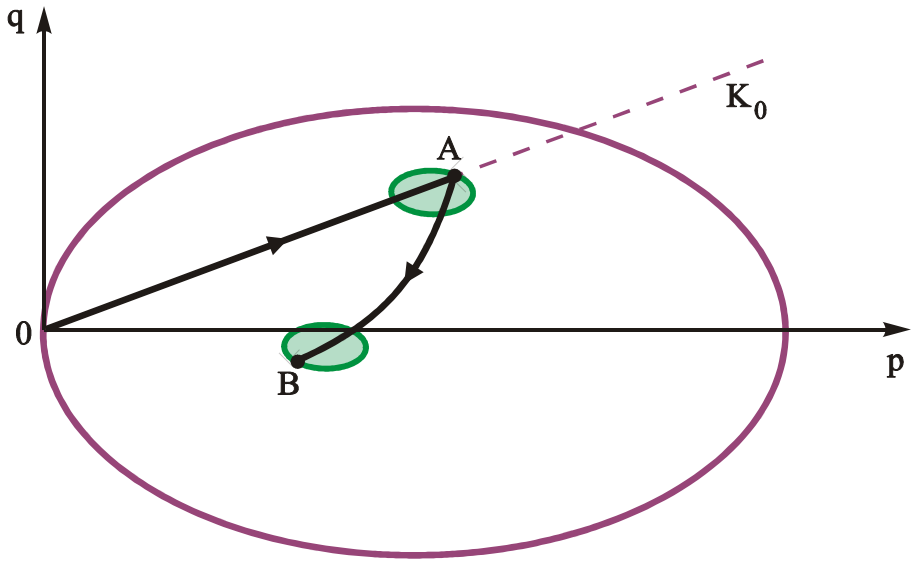

Figura 3: Overconsolidation process in the modified model (mobile projection centre).

3 MODEL WITH MOBILE PROJECTION CENTER

Although the initial general formulation of the bounding surface model was based on the assumption the existence of a mobile projection centre [9], the various specific formulations presented use a fixed projection centre located on the isotropic axis [10]. Here, it is proposed that the projection centre is able to move, pursuing the stress state, according to:

$$\dot{\mathbf{a}} = c_a \left\| \dot{\boldsymbol{\varepsilon}}^i \right\| (\boldsymbol{\sigma} - \mathbf{a}) \tag{2}$$

where $\dot{\boldsymbol{\varepsilon}}^i$ is the inelastic strain rate (plastic plus viscoplastic) and c_a is a model constant that controls the velocity of translation. This change implies several modifications in the model's formulation. Namely, the expressions for the plastic multiplier, the hardening function, the projection of the stress state into the bounding surface and the plastic modulus. The proposed changes have been implemented and confronted with experimental results, as will be shown in the next section.

Some numerical experiments simulating a conventional drained triaxial test on virtual soil with an unloading/reloading cycle were carried out in [1] and are shown in Figures 4 and 5. Figure 4 shows the stress-strain curves for different strain rates. In Figure 5, the first loading phase takes place at a strain rate equal in all tests (2×10^{-6} s^{-1}), with the unloading and reloading stages taking place at different strain rates. In both cases, the loading and reloading stages exhibit an expected increase in stress with the strain rate, with the upper limit being the elastoplastic behaviour. During unloading the stress decreases with increasing strain rate. Theses examples illustrate that, unlike the formulation with a fixed projection centre, this model can reproduce closed loops for relatively small variations of deviatoric stress, which

remains positive, as observed experimentally.

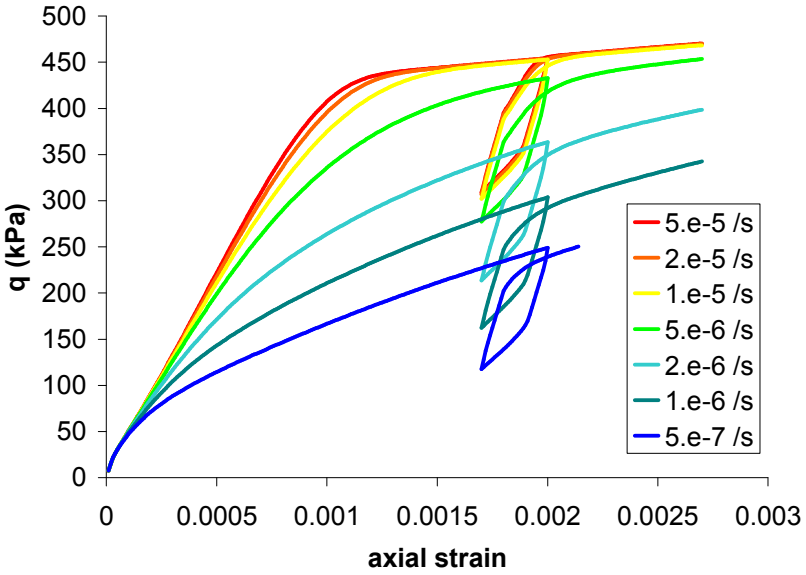

Figure 4: Drained triaxial tests for different strain rates (models with mobile projection centre).

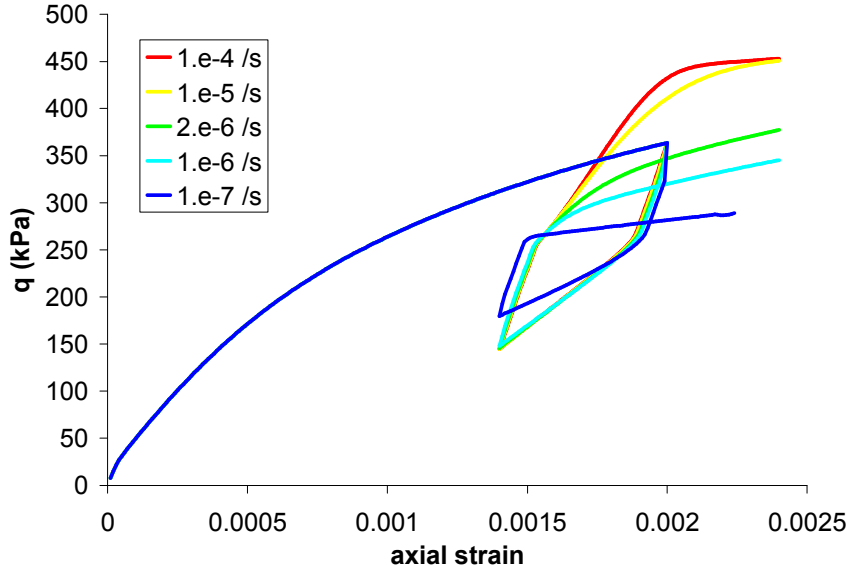

Figure 5: Drained triaxial tests with different strain rates in the unloading-reloading stages (model with mobile projection centre).

4 CYCLIC CREEP TEST. RESULTS AND NUMERICAL SIMULATION

4.1 Main characteristics of *Formação de Benfica* clay

The test carried out to study the model proposed in this work was carried out in the *Formação de Benfica* overconsolidated stiff clays, a significant geological formation within

the Lisbon region. This tested sample is a structured soil with an ASTM classification of SC with an IP of 35.4% and LL of 61.4% and low permeability (2×10^{-10} m/s).

4.2 Loading sequence

The imposed loading sequence involved a series of unloading steps followed by a series of reloading steps, with each step consisting first in a relatively fast change in deviatoric stress (aprox. 6×10^{-6} s^{-1} strain rate) followed by 24h creep at constant deviatoric stress and constant total mean stress. The loading sequence was carried out in undrained conditions.

After the monotonic deviatoric loading up to q=250kPa, during the unloading sequence, the creep strains increased in the reverse direction (Figure 6), *i.e.*, for the highest q values, the creep strains are lower and progressively increase with decreasing q. When the deviatoric stress attains zero, significant creep strains are observed. Conversely, during the reloading sequence, with q increasing from 0 to 250kPa, the creep strains increase with increasing q values with significant large creep strains for q=250kPa. It is however important to note that during initial loading sequence a situation corresponding to tertiary creep (failure) was not achieved.

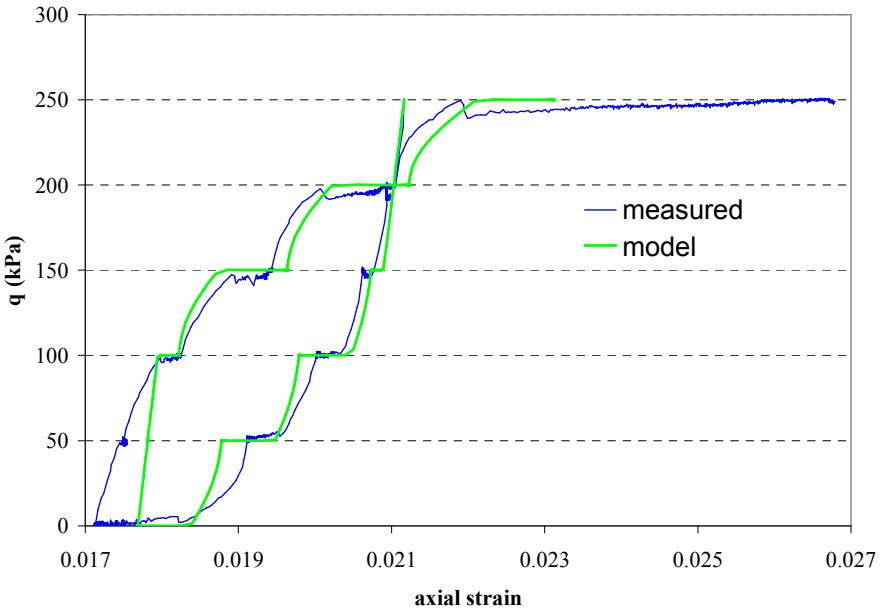

Figure 6: Unloading-reloading steps with creep stages in undrained triaxial test with constant p (measured – blue line, model with mobile projection centre – green line).

4.3 Numerical simulation

Some elements already available from previous studies on samples of this formation were used in the calibration of the model. This calibration was performed for a single unloading-reloading cycle and its aim was to reproduce qualitatively the most significant aspects observed in the experiment. A set of material constants was chosen from a large series of analyses made by randomly varying a set of five parameters affecting viscous behaviour that

produced a best fit to the measured stress-strain curve. The adjustment shown in Figure 6 has been achieved for the following material constant values: V=5×10^9 , s_v=1.12 , c_a=652 , n=2.1 and α=0.

It is important to note that a constitutive model with a fixed projection centre cannot even qualitatively reproduce the type of behaviour exhibited in this test.

The effective stress path and snapshots of the projection centre (whose speed can be controlled by the constant c_a) with the corresponding viscous nucleus at different instants are shown in Figure 7. The instants represented are the end of the isotropic consolidation stage, the end of the first unloading step and after the following creep stage, the end of the last unloading step and after the following creep stage, and the end of the last reloading step as well as the end of the next creep stage. The projection centre (and the viscous nucleus) follows the stress state. During the loading steps, due to the high rate of loading, the projection centre lags behind the stress state and consequently the stress moves outward from the viscous nucleus boundary. During the creep stages the projection centre approaches the stress state until the viscous nucleus's boundary catches the latter at which point the creep strains cease. In the case of the first unloading step, the stress moves to the inside of the viscous nucleus, the response is entirely elastic and the projection centre doesn't move. It should be mentioned that some viscous strains may also occur during the loading stages.

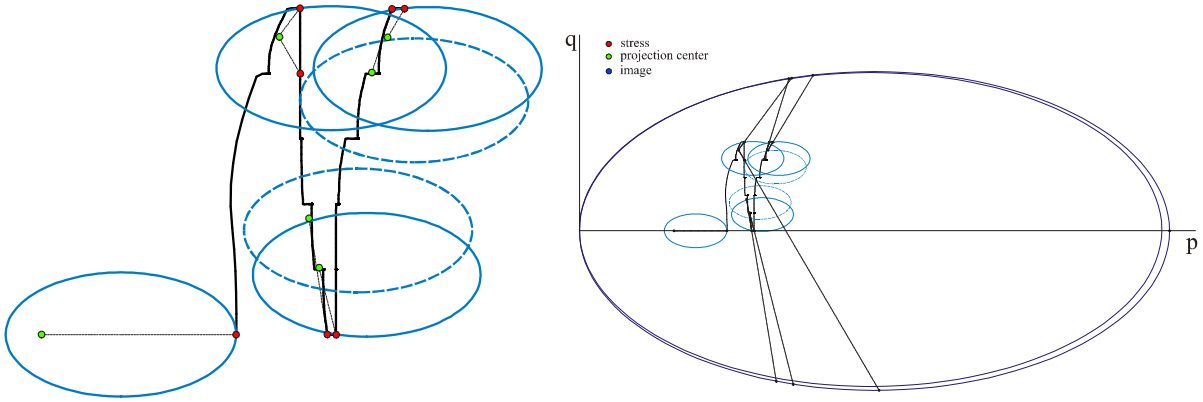

Figure 7: Computed effective stress path. Viscous nuclei at the end of isotropic consolidation, first unloading step, last unloading step and last reloading step. At the beginning (broken line) and the end of the creep stage (full line). Stress points (red). Projection centres (green). The global view on the right side includes image points (blue) on the bounding surface.

Results of the measured and computed pore pressures histories are shown in Figure 8. The model, as it stands, is not able to reproduce, even qualitatively, the observed pore pressure response. The model predicts pore pressure decreases during unloading, in contradiction with the measurements that show a pore pressure increase. This is one aspect of the model that needs to be improved. During reloading the model predicts decreasing pore pressures whose magnitude increases with the deviatoric stress level. This is in qualitative agreement with the measurements.

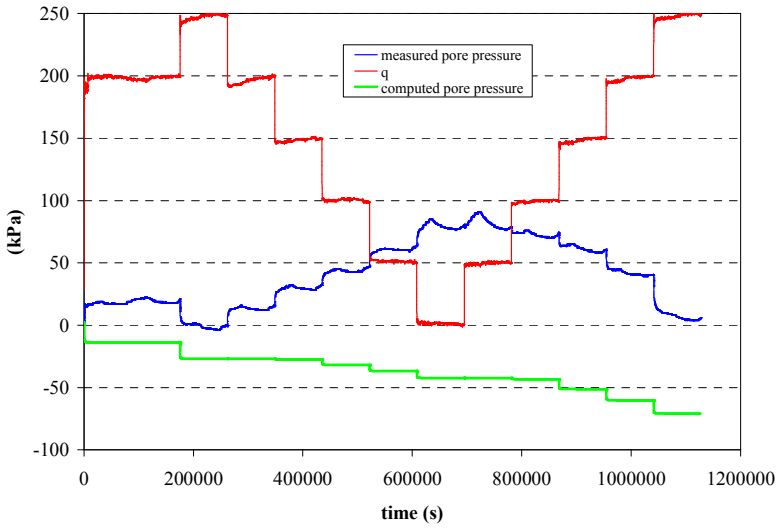

Figure 8: History of measured (blue line) and computed (green line) pore pressures. Applied deviatoric stress history (red line).

As the pore pressure variations reflect the inelastic volumetric strains, and assuming an associated flow rule, the inability of the model to reproduce the pore pressure changes with loading might be an indication that the shape of the bounding surface is not suitable. A sheared elliptical shape such as used to model anisotropic plastic response in soils [11] would produce, at least qualitatively, correct pore pressure variations as illustrated in Figure 9.

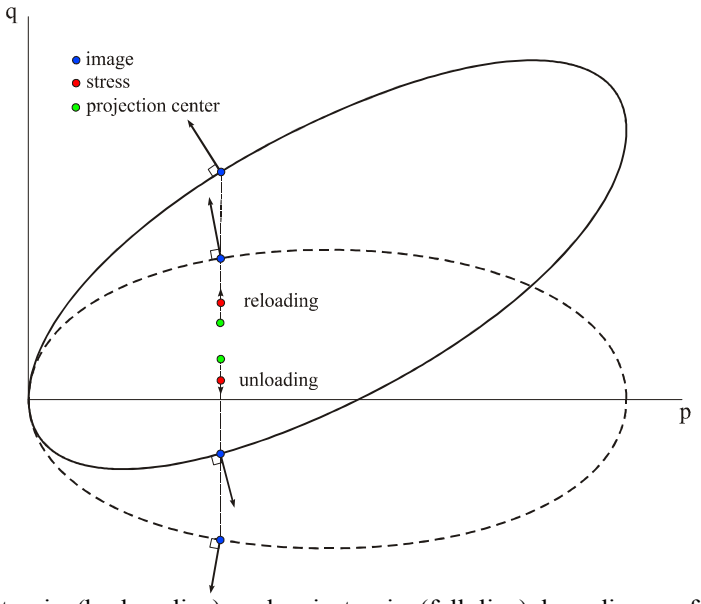

Figure 9: Isotropic (broken line) and anisotropic (full line) bounding surfaces with associated flow rule during unloading and reloading.

In the case of the sheared ellipse there is a region, from slightly to medium

overconsolidated states, inside which the sign of the pore pressure change response agrees with the measured. As can be seen in Figure 9 for the unloading situation, the projection of the normal to the anisotropic bounding surface on the isotropic axis has opposite direction to the one given by the isotropic bounding surface. This suggests that the anisotropic nature of the soil cannot be ignored if the correct volumetric response is to be achieved by the model.

5 CONCLUSIONS

In this work, a new model that takes into account the cyclic time behaviour of soils has been proposed. Some inconsistencies between observed soil behaviour and the response given by models for rate dependent soils have been described. These inconsistencies have been solved with a mobile projection centre that approaches the stress state with some delay and as such is able to develop viscous (including creep) strains.

The response of the improved model has been compared with that of a triaxial undrained test during an unloading/reloading deviatoric stress cycle at constant total mean stress that incorporated a series of staggered fast loading steps and creep stages. A reasonable agreement with the measured response has been obtained. The model has clearly been able to qualitatively reproduce the main observed aspects of the stress-strain response of a stiff overconsolidated clay under a stress loading cycle with creep stages.

One aspect that the model has not been able to reproduce is the observed pore pressure evolution. It has been suggested that the adoption of an anisotropic bounding surface with an associated flow can improve the model in this respect.

Another aspect that might improve the model concerning this type of soils is the incorporation of destructuring.

REFERENCES

[1] Maranha, J. R. and Vieira, A. (2010). Formulação de um centro de projecção móvel num modelo elastoplástico-viscoplástico para solos. *12º Congresso Nacional de Geotecnia*, Guimarães, Portugal.

[2] Kaliakin, V. N. and Dafalias, Y. F. (1990). Theoretical Aspects of the Elastoplastic-Viscoplastic Bounding Surface Model for Cohesive Soils. *Soils and Foundations*, Vol. 30, No. 3, 11-24

[3] Kaliakin, V. N. and Dafalias, Y. F. (1990a). Verification of the Elastoplastic-Viscoplastic Bounding Surface Model for Cohesive Soils. *Soils and Foundations*, Vol. 30, No. 3, 25-36.

[4] Hashiguchi, K. and Okayasu, T. (2000). Time-Dependent Elastoplastic Constitutive Equation Based on the Subloading Surface Model and Its Application to Soils. *Soils and Foundations*, Vol. 40, No. 4, 19-36.

[5] Vieira, A.M. (2006*). Estudo do Comportamento Diferido no Tempo de Túneis em Argilas Sobreconsolidadas.* Tese de Doutoramento, Faculdade de Ciências e Tecnologia da Universidade de Coimbra.

[6] Maranha, J. and Vieira, A. (2005). Modelling the time dependent behaviour of a tunnel using a elastoplastic-viscoplastic model. *Proceedings of the 8th International Conference on Computational Plasticity, COMPLAS VIII, Barcelona.*

[7] Vieira, A., Maranha, J., Bilé Serra, J. and Correia, R. (2007). Modelling the undrained creep behaviour of a hard clay in the super-critical region. (Eds. E. Oñate, D.R.J. Owen and B. Suárez), *Proceedings of the 9th International Conference on Computational Plasticity, COMPLAS IX, Barcelona*, pp. 836 – 839.
[8] Chaboche, J. L. (1977). Viscoplastic Constitutive Equations for the Description of Cyclic and Anisotropic Behaviour of Metals. *Bulletin de L'Academie Polonaise des Sciences*, Vol. 25-1, 33-39.
[9] Dafalias, Y. F. (1986). Bounding Surface Plasticity. I: Mathematical Foundation and Hypoplasticity. *Journal of Engineering Mechanics*, Vol. 112, No. 9, 966-987.
[10] Dafalias, Y. F. and Herrmann, L. R. (1986). Bounding Surface Plasticity. II: Application to Isotropic Cohesive Soils. *Journal of Engineering Mechanics*, Vol. 112, No. 12, 1263-1261.
[11] Whittle A. J. and Kavvadas M. J. (1994). Formulation of MIT-E3 constitutive model for overconsolidated clays. *Journal of Geotechnical Engineering*, ASCE, 120:173-198.